PROBLEM OF PHYSICAL NON-REALIZABILITY OF SOME EQUIVALENT CURRENTS AMPLITUDE DISTRIBUTIONS FEEDING SLOTS IN WAVEGUIDE ANTENNAS

By Michal Grabowski

Cobham Antenna Systems (Marlow)

Abstract

In this paper the Full-Wave design method of the non-resonant waveguide multi-slots antenna is presented. The internal mutual couplings between adjacent radiating slots are considered in the described method. The problem of the physical non-realizability of some equivalent currents amplitude distributions feeding slots, caused by the internal mutual couplings between slots is also presented. Some corrective solutions which allow solving mentioned problem are proposed. In order to confirm the usefulness of the presented solutions the obtained results are compared to their equivalents reached in computer simulations with the use of CST Microwave Studio.

1 Introduction

The non-resonant waveguide multi-slots antennas (see Fig. 1) are passive radiating structures which are commonly used in the microwave transmitter and receiver devices. Such antennas radiate energy from a feeding waveguide to a free space through longitudinal slots cut in a broad or narrow wall of an air rectangular waveguide. The special interest of such antennas is caused by their planar and compact structure, a high power handling capacity and electrical parameters, such as a high efficiency, a relatively wide frequency band and a good return loss. Their additional advantage is the ability to combine vertical slotted waveguides as a phased array with shaped and electronically switched multi-beam radiation patterns, which enables to observe many moving targets at the same time. The advantages mentioned above cause that these antennas are a subject of many publications such as [1][2][4][5][6][7][15].

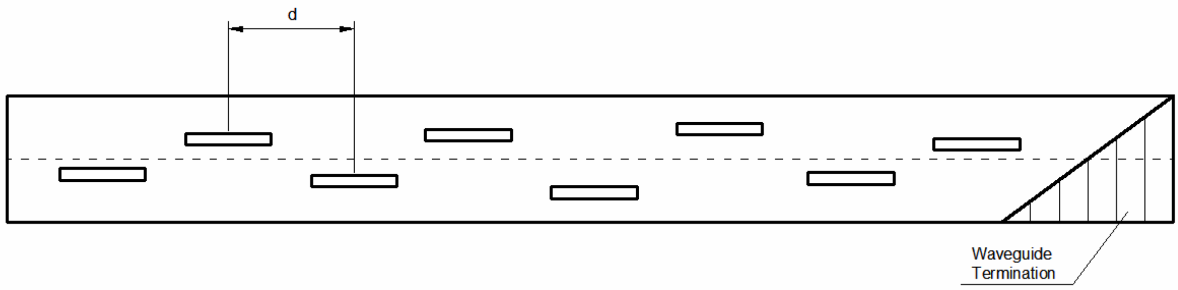

Figure 1. The non-resonant waveguide antenna with longitudinal slots.

The waveguide multi-slots antennas might be realized both as a resonant (distance between adjacent slots equals to the half waveguide wavelength) and non-resonant (distance between adjacent slots different than the half waveguide wavelength) [2][8][9][10][12][15][16][18]. Among antennas from a non-resonant subgroup it is possible to distinguish antennas which work over or below the resonant frequency (respectively distance between adjacent slots smaller or larger than the half waveguide wavelength). The non-resonant waveguide multi-slots antennas, which are tipped with a waveguide termination, are characteristics of an effect of squint (non-occurring for the resonant ones). This effect causes an angle deviation of an end fire direction from a normal to an antenna aperture. Additionally this deviation is depended on an operating frequency and is described as:

$$\theta_0 = \arcsin\left(\frac{\psi_0 \cdot \lambda}{2\pi d}\right) \quad (1)$$

where ψ_0 is a phase difference of currents feeding nearby slots, while d is a physical distance between adjacent slots.

Presenting antennas are commonly used in radiolocation devices. In these applications it is desirable to transmit and receive energy to and from a narrow sector of a free space. This requirement is realized by combining several identical parallel rectangular waveguide antennas with close to half-wave slots cut in their walls [8][9][10][15]. Radiation patterns of such antennas are depended on complex amplitude distributions of equivalent currents feeding slots (currents corresponding to surface currents superposition which flows over walls of waveguide and crossing slots). Appropriate amplitude distributions of currents fed radiating slots are determined during the synthesis process for a definite spatial radiation pattern. Multi-slots array spatial radiation patterns might be determined by several methods, described in literature [1][11][15], such as: Taylor, Dolph-Tschebyshev or Fourier Integral Methods.

The design of the slotted waveguide array antenna is a fairly complicated task. It is required to include an influence of the internal (by a supplying slots waveguide) and the external (through the open space) mutual couplings between radiating slots on a radiation pattern. Such mutual couplings are deforming a radiation pattern of an array antenna as a rule, what can be mostly seen as a side lobes level increased, widen of a main lob and an angle deviation of an end fire direction from a normal to an antenna aperture. In an extreme situation it can lead to an antenna physical non-realizability. It causes the necessity of change in a desirable shape of an antenna radiation pattern, increase of the antenna loss coefficient or the need to use a complicated configuration of the antenna feeding structure.

In this paper to determine an influence of the internal mutual couplings effect between slots on the radiation pattern, the Full-Wave method is used. Case, when the mutual couplings effect between slots is making the physical non-realizability of the antenna for particular amplitude distributions of currents feeding slots, is also presented. There are shown some solutions, which helps to solve the problem of the antenna non-realizability for currents distributions. The proposed solutions are a little modification of the loss coefficient, an adjustment of the feeding slots current distributions and an increase a number of slots. Radiation patterns obtained with the Full-Wave method are compared to their equivalents reached of computer simulations with the use of CST Microwave Studio.

2 The Full-Wave method design of slotted waveguide antennas included the internal mutual couplings between slots

The design of multi-slots waveguide antenna requires determining of slots geometric dimensions and their location in a waveguide depended on amplitude distributions of equivalent feeding slots currents. Such antennas can be analyzed by various methods. The easiest Energetic Method is described in [15]. Unfortunately, it doesn't take into consideration the effect of the internal mutual couplings between slots. It causes that results are encumbered with errors. The Full-Wave Method, which includes the internal mutual couplings between slots is definitely more precise to the waveguide antenna design. The presented Full-Wave Method is extended by a correction stage, in which an influence of non-resonant slot lengths on the radiation patterns is also taken into consideration. This Method enables to obtain the radiation pattern of an antenna for the determined current amplitude distribution and the loss coefficient χ_N (means as an energy lost in a waveguide termination). In this paper only a short presentation of this method is presented. Full descriptions of this method with examples of the usage are shown in [8][9][10][16].

Algorithm of the Full-Wave Method, extended by correction stage including non-resonant slot lengths

As mentioned above, in the non-resonant antennas distances between adjacent slots d are different than $\lambda_{01}/2$, where λ_{01} is a waveguide wavelength. Such antennas are tipped with the waveguide terminations, which causes that wave propagating in a waveguide is close to the travelling wave. In Fig. 2 are shown the three basic solutions of the slotted waveguide antennas. Respectively there are antennas with longitudinal slots cut in a broad wall (Fig. 2a), and inclined slots cut in a broad (Fig. 2b) and a narrow wall (Fig. 2c) of a rectangular waveguide.

a)

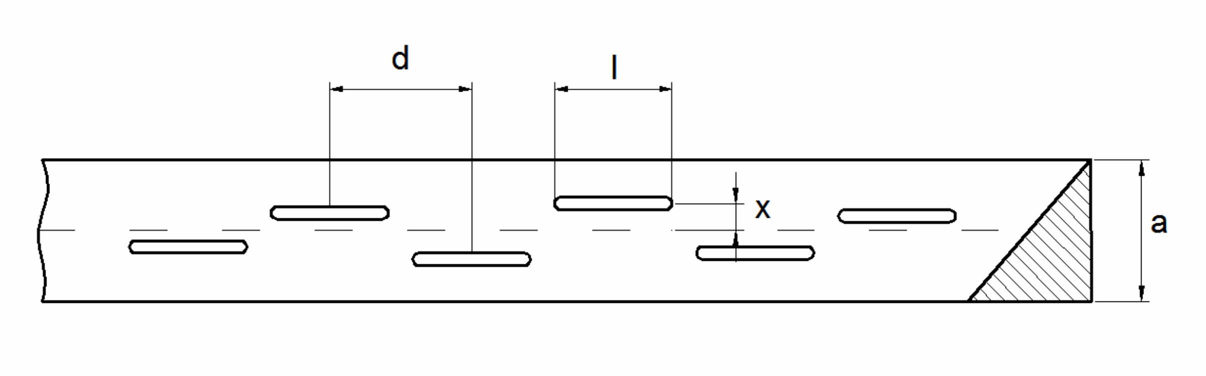

b)

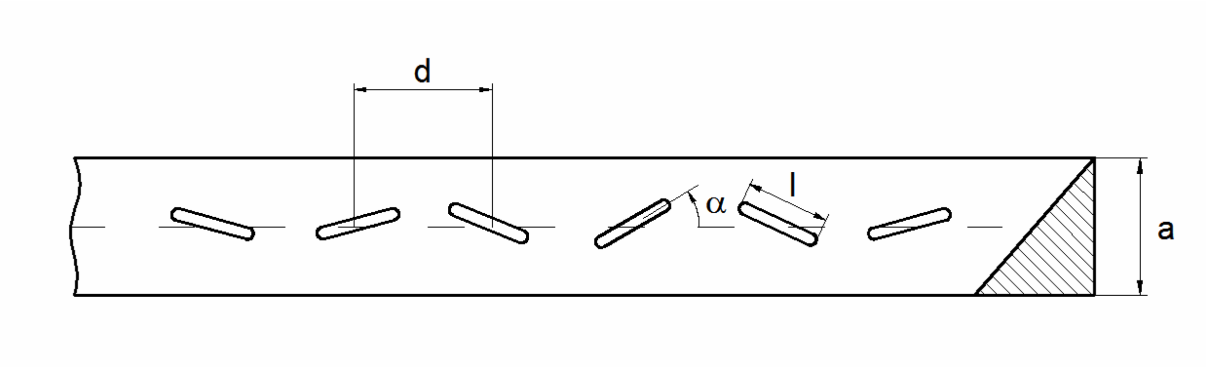

c)

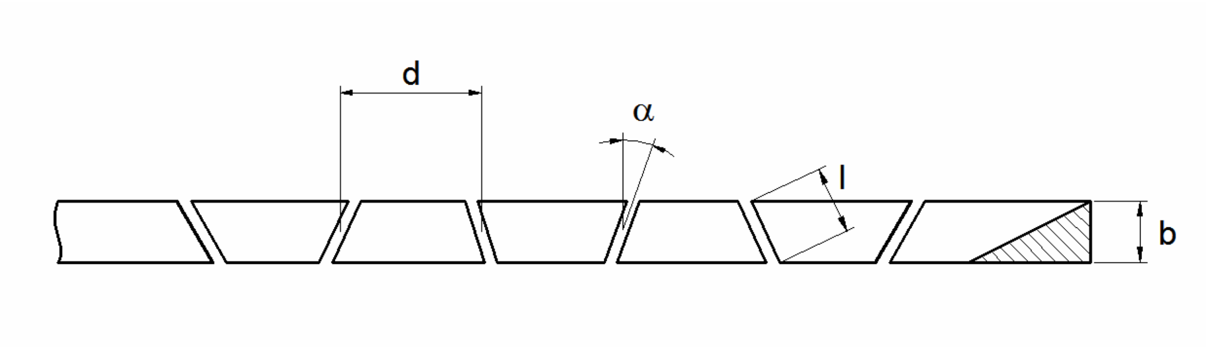

Figure 2. Basic solutions of the slotted waveguide antennas with: (a) longitudinal slots, (b) inclined slots cut in a broad wall, (c) inclined slots cut in a narrow wall.

In order to reach an optimal coupling of slots and feeding waveguide, lengths of all slots near to the resonant length are desired (typically it is $l \in \langle 0.9 \cdot l_r \text{ , } 1.1 \cdot l_r \rangle$). By the resonance frequency is assumed the frequency when imaginary part of an impedance or an admittance represented the slot, equals zero, [17]. So for resonance slots their impedances or admittances are real values.

The Full–Wave Method enables to design antennas including the internal mutual couplings between slots. This method extended by a correction stage including the non-resonant slot lengths takes into consideration an influence of slots susceptance or reactance in case their lengths are different then resonant length ($l \neq l_r$), on the radiation pattern. The basis of this method is to evaluate partial reflections of the electromagnetic wave from succeeding slots which cause a considerable displacement of the EM field inside the waveguide. An essential problem of this approach is to calculate a complex amplitude distribution of waves propagating from the waveguide input to the matched termination and in the reverse direction (see Fig. 3). Dependently on slot types such structures can be analyzed as different equivalent circuits. For inclined slots cut in a broad wall of rectangular waveguide (see Fig. 2b) each of these slots become the serial lumped impedances. On the contrary longitudinal shunt slots cut in a broad wall (see Fig. 2a) and inclined slots cut across a narrow wall (see Fig. 2c) can be determined as parallel admittances inserted in a waveguide. Equivalent circuit of the N-slotted waveguide antenna, where each slot is represented by a normalized parallel admittance ($y_k = Y_k / Y_0 = g_k + jb_k$) inserted into a long transmission line with a characteristic admittance Y_0, is shown in Fig. 3a. Respectively in Fig. 3b is presented an equivalent circuit of the N-slotted waveguide antenna, where each slot is represented by normalized serial impedance ($z_k = Z_k / Z_0 = r_k + jx_k$) inserted into a long transmission line with a characteristic impedance Z_0.

a)

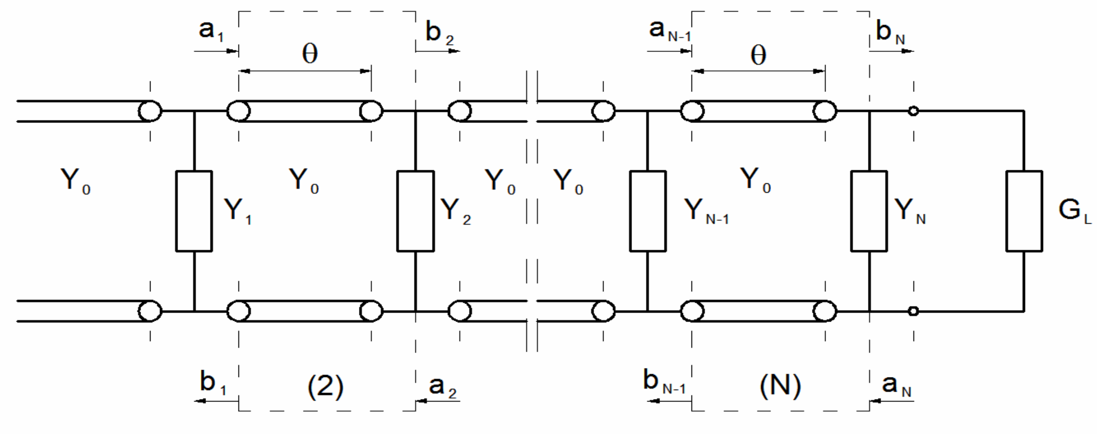

b)

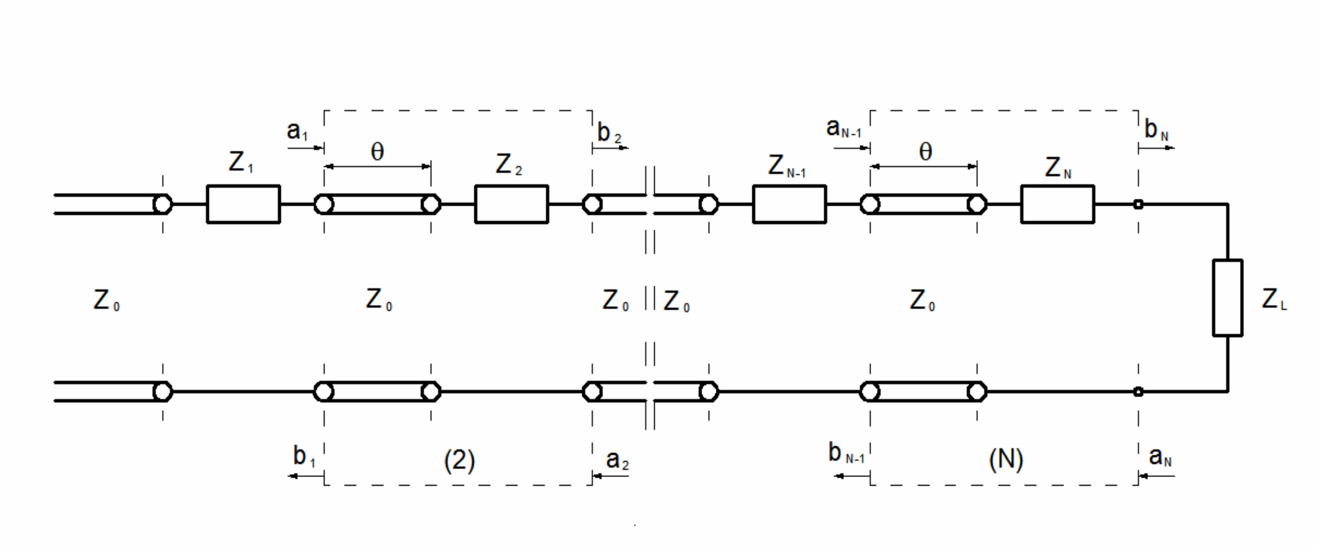

Figure 3. Electrical schemes of the N-slotted waveguide antennas equivalent circuits, with slots represented by normalized (a) parallel admittance or (b) serial impedance inserted into a long transmission line.

Circuits shown in Fig. 3. can be analyzed as a cascade connection of the N two-port substitute circuits shown in Fig. 4.

a) *b)*

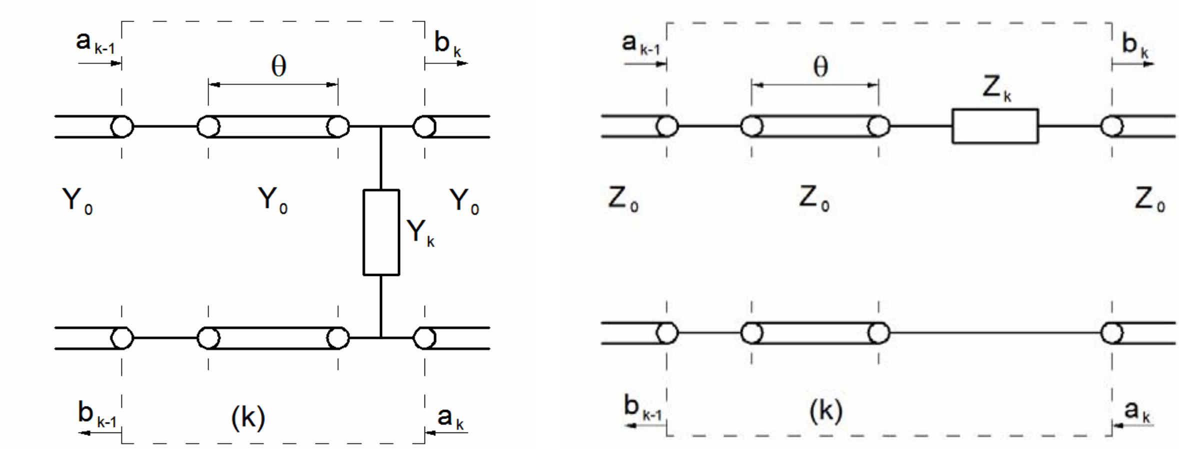

Figure 4. Electrical schemes of the two-port substitute circuits where slot is represented by (a) parallel admittance or (b) serial impedance inserted into a long transmission line.

The transmission matrix **T** of the circuit shown in Fig. 4 equals to the product of the transmission matrixes of a long transmission line with a characteristic admittance Y_0 and a parallel inserted normalized admittance y_k (see Fig. 4a) or serially inserted normalized impedance z_k (see Fig. 4b). The transmission matrix of the circuit, shown in Fig. 4a, equals ([8][9][10][16]):

$$\begin{bmatrix} T_{11}^{(k)} & T_{12}^{(k)} \\ T_{21}^{(k)} & T_{22}^{(k)} \end{bmatrix} = \frac{1}{2} \begin{bmatrix} \cos\theta - j\sin\theta & 0 \\ 0 & \cos\theta + j\sin\theta \end{bmatrix} \cdot \begin{bmatrix} 2 - g_k - jb_k & -g_k - jb_k \\ g_k + jb_k & 2 + g_k + jb_k \end{bmatrix} \tag{2}$$

After multiplication Equation (2) equals:

$$\begin{aligned}
T_{11}^{(k)} &= \left(1 - \frac{g_k}{2}\right)\cos(\theta) - \frac{b_k}{2}\sin(\theta) - j\left[\left(1 - \frac{g_k}{2}\right)\sin(\theta) + \frac{b_k}{2}\cos(\theta)\right] \\
T_{12}^{(k)} &= -\frac{g_k}{2}\cos(\theta) - \frac{b_k}{2}\sin(\theta) + j\left[\frac{g_k}{2}\sin(\theta) - \frac{b_k}{2}\cos(\theta)\right] \\
T_{21}^{(k)} &= \frac{g_k}{2}\cos(\theta) - \frac{b_k}{2}\sin(\theta) + j\left[\frac{g_k}{2}\sin(\theta) + \frac{b_k}{2}\cos(\theta)\right] \\
T_{22}^{(k)} &= \left(1 + \frac{g_k}{2}\right)\cos(\theta) - \frac{b_k}{2}\sin(\theta) + j\left[\left(1 + \frac{g_k}{2}\right)\sin(\theta) + \frac{b_k}{2}\cos(\theta)\right]
\end{aligned} \tag{3}$$

Respectively the transmission matrix for the two-port circuit shown in Fig. 4b, equals ([8][9][10][16]):

$$\begin{bmatrix} T_{11}^{(k)} & T_{12}^{(k)} \\ T_{21}^{(k)} & T_{22}^{(k)} \end{bmatrix} = \frac{1}{2} \begin{bmatrix} \cos\theta - j\sin\theta & 0 \\ 0 & \cos\theta + j\sin\theta \end{bmatrix} \cdot \begin{bmatrix} 2 - r_k - jx_k & r_k + jx_k \\ -r_k - jx_k & 2 + r_k + jx_k \end{bmatrix} \tag{4}$$

Elements of this matrix may be given by:

$$\begin{aligned}
T_{11}^{(k)} &= \left(1 - \frac{r_k}{2}\right)\cos(\theta) - \frac{x_k}{2}\sin(\theta) - j\left[\left(1 - \frac{r_k}{2}\right)\sin(\theta) + \frac{x_k}{2}\cos(\theta)\right] \\
T_{12}^{(k)} &= \frac{r_k}{2}\cos(\theta) + \frac{x_k}{2}\sin(\theta) + j\left[\frac{x_k}{2}\cos(\theta) - \frac{r_k}{2}\sin(\theta)\right] \\
T_{21}^{(k)} &= -\frac{r_k}{2}\cos(\theta) + \frac{x_k}{2}\sin(\theta) - j\left[\frac{r_k}{2}\sin(\theta) + \frac{x_k}{2}\cos(\theta)\right] \\
T_{22}^{(k)} &= \left(1 + \frac{r_k}{2}\right)\cos(\theta) - \frac{x_k}{2}\sin(\theta) + j\left[\left(1 + \frac{r_k}{2}\right)\sin(\theta) + \frac{x_k}{2}\cos(\theta)\right]
\end{aligned} \tag{5}$$

According to the Fig. 4 all incident and reflected waves at the input of the *k*th-circuit are related to the appropriate waves at the output of this circuit through the following simple formula:

$$\begin{bmatrix} b_{k-1} \\ a_{k-1} \end{bmatrix} = \begin{bmatrix} T_{11}^{(k)} & T_{12}^{(k)} \\ T_{21}^{(k)} & T_{22}^{(k)} \end{bmatrix} \cdot \begin{bmatrix} a_k \\ b_k \end{bmatrix} \tag{6}$$

Where a_{k-1}, b_{k-1} are the complex amplitudes of the incident and reflected waves at the input of the *k*th-circuit and a_k, b_k are the complex amplitudes of the reflected and incident waves at the output of this circuit. Complex amplitudes at the output of the *k*th-circuit equal:

$$b_{k-1} = T_{11}^{(k)} \cdot a_k + T_{12}^{(k)} \cdot b_k$$
$$a_{k-1} = T_{21}^{(k)} \cdot a_k + T_{22}^{(k)} \cdot b_k \qquad (7)$$

For $a_{k-1} = A_{k-1} + jB_{k-1}$, $b_{k-1} = C_{k-1} + jD_{k-1}$, $a_k = A_k + jB_k$ and $b_k = C_k + jD_k$, Equation (7) is given as follows ([8][9][10][16]):

$$C_{k-1} + jD_{k-1} = T_{11}^{(k)}(A_k + jB_k) + T_{12}^{(k)}(C_k + jD_k)$$
$$A_{k-1} + jB_{k-1} = T_{21}^{(k)}(A_k + jB_k) + T_{22}^{(k)}(C_k + jD_k) \qquad (8)$$

According to Equations (3) and (8) (respectively for the slots represented by the transmission line with the parallel inserted normalized admittances) the parameters A_{k-1}, B_{k-1}, C_{k-1} and D_{k-1} take the following forms:

$$A_{k-1} = \left(1 + \frac{g_k}{2}\right)[C_k \cos(\theta) - D_k \sin(\theta)] + \frac{g_k}{2}[A_k \cos(\theta) - B_k \sin(\theta)] +$$
$$- \frac{b_k}{2}[A_k \sin(\theta) + B_k \cos(\theta) + C_k \sin(\theta) + D_k \cos(\theta)]$$

$$B_{k-1} = \left(1 + \frac{g_k}{2}\right)[C_k \sin(\theta) + D_k \cos(\theta)] + \frac{g_k}{2}[A_k \sin(\theta) + B_k \cos(\theta)] +$$
$$+ \frac{b_k}{2}[A_k \cos(\theta) - B_k \sin(\theta) + C_k \cos(\theta) - D_k \sin(\theta)] \qquad (9)$$

$$C_{k-1} = \left(1 - \frac{g_k}{2}\right)[A_k \cos(\theta) + B_k \sin(\theta)] - \frac{g_k}{2}[C_k \cos(\theta) + D_k \sin(\theta)] +$$
$$- \frac{b_k}{2}[A_k \sin(\theta) - B_k \cos(\theta) + C_k \sin(\theta) - D_k \cos(\theta)]$$

$$D_{k-1} = \left(1 - \frac{g_k}{2}\right)[-A_k \sin(\theta) + B_k \cos(\theta)] + \frac{g_k}{2}[C_k \sin(\theta) - D_k \cos(\theta)] +$$
$$- \frac{b_k}{2}[A_k \cos(\theta) + B_k \sin(\theta) + C_k \cos(\theta) + D_k \sin(\theta)]$$

For the waveguide antennas represented by the transmission line with serially inserted normalized impedances, Equations (9) are as follows:

$$A_{k-1} = \left(1 + \frac{r_k}{2}\right)[C_k \cos(\theta) - D_k \sin(\theta)] - \frac{r_k}{2}[A_k \cos(\theta) - B_k \sin(\theta)] +$$
$$+ \frac{x_k}{2}[A_k \sin(\theta) + B_k \cos(\theta) - C_k \sin(\theta) - D_k \cos(\theta)]$$

$$B_{k-1} = \left(1 + \frac{r_k}{2}\right)[C_k \sin(\theta) + D_k \cos(\theta)] - \frac{r_k}{2}[A_k \sin(\theta) + B_k \cos(\theta)] +$$
$$- \frac{x_k}{2}[A_k \cos(\theta) - B_k \sin(\theta) - C_k \cos(\theta) + D_k \sin(\theta)] \qquad (10)$$

$$C_{k-1} = \left(1-\frac{r_k}{2}\right)\left[A_k \cos(\theta)+B_k \sin(\theta)\right]+\frac{r_k}{2}\left[C_k \cos(\theta)+D_k \sin(\theta)\right]+$$

$$-\frac{x_k}{2}\left[A_k \sin(\theta)-B_k \cos(\theta)-C_k \sin(\theta)+D_k \cos(\theta)\right]$$

$$D_{k-1} = \left(1-\frac{r_k}{2}\right)\left[-A_k \sin(\theta)+B_k \cos(\theta)\right]-\frac{r_k}{2}\left[C_k \sin(\theta)-D_k \cos(\theta)\right]+$$

$$-\frac{x_k}{2}\left[A_k \cos(\theta)+B_k \sin(\theta)-C_k \cos(\theta)-D_k \sin(\theta)\right]$$

The design of the N-slotted waveguide antenna with the Full-Wave Method is realized for the determined power amplitude distribution P_k radiated by each slot (this amplitudes should be normalized to the input power P_0). The loss coefficient χ_N defined as the ratio between power lost in the matched termination and the input power must be also determined. Typical value of the loss coefficient χ_N is chosen from a range $0.05 \le \chi \le 0.2$. For the determined power amplitude distribution P_k it is possible to recalculate normalized values of the conductance or resistance for all slots. The conductance of the *k*th-slot, which the equivalent circuit is shown in Fig. 4a and is defined as:

$$g_k = \frac{P_k}{\left|a_k + b_k\right|^2} = \frac{P_k}{(A_k + C_k)^2 + (B_k + D_k)^2} \tag{11}$$

where A_k, B_k, C_k and D_k are determined in Equation (9).

The phase of the equivalent current flows through the *k*th-slot equals ([8][9][10][16]):

$$\phi_k = \arg(a_k + b_k) = arctg\left(\frac{B_k + D_k}{A_k + C_k}\right) + m \cdot \pi \tag{12}$$

where $m = 1,2,3,...$. Parameter m is chosen in that way to minimise the phase deviation ϕ_k from the linear distribution. Similarly, the *k*th-slot resistance, which the equivalent circuit is shown in Fig. 4b, may be reached by the following formula:

$$r_k = \frac{P_k}{\left|b_k - a_k\right|^2} = \frac{P_k}{(C_k - A_k)^2 + (D_k - B_k)^2} \tag{13}$$

The phase angle of the complex equivalent current amplitude, which flows through resistances representing considered slots, is given by the equation:

$$\phi_k = \arg(b_k - a_k) = arctg\left(\frac{D_k - B_k}{C_k - A_k}\right) + n \cdot \pi \tag{14}$$

where $n = 0,1,2,...$.

The Full-Wave method of the antenna analysis begins from the last *N*th-circuit. Let us assume that the waveguide is loaded with the ideally matched waveguide terminations ($g_{N+1} = r_{N+1} = 1$). Then the absolute square of the amplitude b_N equals to the power lost in matched termination ($|b_N|^2 = \chi_N$) and the amplitude of the wave reflected from the termination equals $a_N = 0$ (see Fig. 3). For this assumption the real and imaginary amplitudes of the incident and reflected waves for the waveguide termination equal: $A_N = 0$, $B_N = 0$, $C_N = \sqrt{\chi}$, $D_N = 0$. Conductance of the *N*th-slot (see Fig. 4a) evaluated with Equation (11) is given as follows ([8][9][10][16]):

$$g_N = \frac{P_N}{C_N^2} = \frac{P_N}{\chi} \tag{15}$$

Respectively resistance of the *N*th-slot shown in Fig. 4b evaluated with Equation (12) equals ([8][9][10][16]):

$$r_N = \frac{P_N}{C_N^2} = \frac{P_N}{\chi} \tag{16}$$

For known conductance or resistance of the *N*th-slot it is possible to determine (with Equation (9) or (10)) real and imaginary parts of incident a_{N-1} and reflected b_{N-1} waves on the input of the *N*th-circuit (see Fig. 3). At the beginning it is needed to assume that reactance and susceptance in Equations (9) or (10) equal zero. For known components A_{N-1}, B_{N-1}, C_{N-1} and D_{N-1}, normalized conductance g_{N-1} or resistance r_{N-1} can be evaluated with Equations (11) or (12). In the analogue way it is possible to evaluate the amplitudes of the incident and reflected waves for the *N-1st*-circuit.

In the similar way conductances or resistances of all slots cut in the antenna can be evaluated. For obtained slots' conductances or resistances it is possible to determine, depended of the slot type, slots structural parameters which are crucial for the coupling between the slot and the feeding waveguide (see Fig. 2). These structural parameters mentioned above are the displacement of a slot from axis of a waveguide x (for the longitudinal slots) and the angle between axis of a slot and axis of a waveguide α (for inclined slots cut in a broad and a narrow wall of a waveguide). Structural parameters can be obtained with proper closed form formulas which are presented in several publications. The most known closed form formulas for slots cut in a waveguide were published by Stevenson in [18]. Unfortunately in these formulas reactance and susceptance of slots are not taken into consideration. The closed form formulas which allow to obtain complex impedance and admittance for a slot cuts in a broad wall were presented by Oliner in [13] and Powen Hsu and Shin H. Chen in [14] for an inclined slot cuts in a narrow wall of a rectangular waveguide. The closed form formulas for an inclined slot cuts in a narrow wall of a rectangular waveguide are also presented in [3].

Slot impedance or admittance, which length is different from resonant, is the complex value and the imaginary part must be taken into account in the antenna design. As mentioned above for the known real part of a slot immitance, structural parameters of these slots with the closed form formulas can be evaluated. During this operation the reactance x_k or the susceptance b_k of all slots are also estimated. In the correction stage (for the non-resonant slot lengths) including imaginary parts of slots' immitance recalculation of the incident and reflected waves for the all *k*th-circuits is required. Components A_k, B_k, C_k and D_k must be recalculated again (with Equation (9) or (10)) where susceptances b_k or reactances x_k equal to the values obtained from the close form formulas. Then conductances (Equation (11)) or resistances (Equation (13)) of all slots can be evaluated again.

The phase of the equivalent current obtained with Equation (12) or (14) flow through all slots enable to determine the deviations of the phase angles from the linear distribution $\delta\phi_k$. This deviation for the *k*th-slot can be given as follows ([8][9][10][16]):

$$\delta\phi_k = \left(\frac{2\pi}{\lambda_{01} d} + \pi\right)(N-k) - \phi_k \tag{17}$$

where ϕ_k is the phase of equivalent current flow through the *k*th-slot.

3 Example of the physical non-realizability of the slotted waveguide antenna for some amplitude distributions of equivalent currents feeding slots in the non-resonant waveguide antenna.

The Full-Wave Method was used to design a non-resonant waveguide antenna with 8 longitudinal slots alternating placed on both sides of a rectangular waveguide's broad wall axis (see Fig. 2b). The waveguide dimensions are as follows: the broad and narrow wall dimensions: $a = 22.86\,\mathrm{mm}$, $b = 10.16\,\mathrm{mm}$, thickness of the wall $t = 1.27\,\mathrm{mm}$ (WR90 waveguide standard). As the desirable Taylor's ([1][11][16]) amplitude distribution of the feeding slots equivalent currents with parameters $\alpha = 2$ and $n = 4$ was chosen. Values of desirable current amplitudes are shown in column 2 of Table I. For calculations assumed: the operation frequency $f_0 = 9.35\,\mathrm{GHz}$, distance between adjacent slots $d = 0.55 \cdot \lambda_g = 24.8\,\mathrm{mm}$ and the loss coefficient $\chi_N = 0.1$ (efficiency coefficient of the antenna equals $\eta = 90\%$). Lengths and widths of slots were chosen in that way to obtain resonant slots. For this assumption slots lengths and widths equal: $L = 15.35\,\mathrm{mm}$ and $W = 1\,\mathrm{mm}$.

Slot No. k	Current Amplitude Distribution I_k	Conductance without Internal Mutual Couplings Consideration g_k	Conductance with Internal Mutual Couplings Consideration g_k	Deviation of the phase angle from linear distribution $\delta\phi_k[°]$
1	0.165	0.0068	0.0030	30.82
2	0.431	0.0468	0.0275	39.81
3	0.767	0.1553	0.1440	44.94
4	1.000	0.3123	0.5120	42.44
5	1.000	0.4541	1.2172	27.94
6	0.767	0.4896	1.2646	9.01
7	0.431	0.3031	0.4584	1.14
8	0.165	0.0637	0.0681	0

Table I. Electrical parameters of the designed antenna

On the basis of the normalized slots conductance obtained with the internal mutual couplings consideration (the Full-Wave Method) it is possible to state that the presented antenna is not physically realized. It is caused because values of normalized conductance for the 5th and 6th slots are larger than 1.0 (see Table I). This fact can be interpreted that the power radiated by these slots should be larger than the power incident to these slots. In Fig. 5 the equivalent voltage amplitude distribution along the feeding waveguide is shown. It is noticeable that in the waveguide there are zones with higher and lower values of electric and magnetic field intensity. These oscillations are caused by wave reflections from individual slots. Centre planes of the first four slots are placed in the waveguide areas for which amplitude of equivalent voltage is close to 1.0. Then these slots radiate the relatively low power in the ratio to the power incident to these slots from the input of the waveguide. Centre planes of the 5th and 6th slots are placed in the waveguide areas with local minimums of the voltage amplitude distribution. These slots must radiate the relatively high power, even larger than the power incident to these slots. It causes that their conductance values are larger than 1.0 and such antenna is not physically realized.

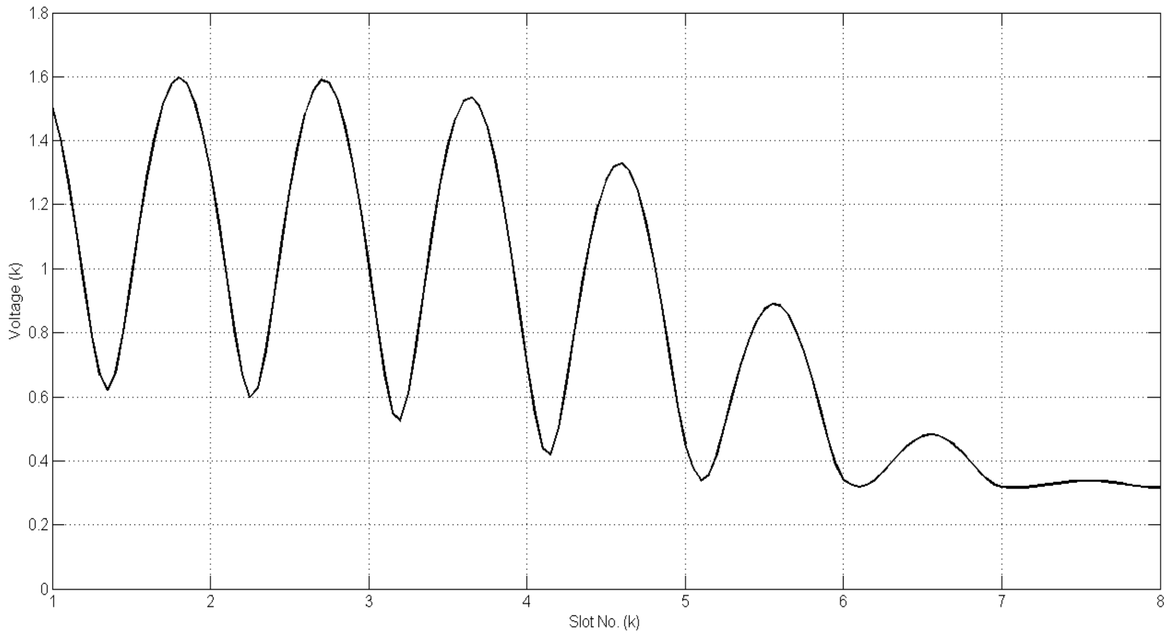

Figure 5. The equivalent voltage amplitude distribution along the feeding waveguide of the designed antenna.

Examples of some corrective solutions which allow solving problem of the physical non-realizability for some amplitude distributions of equivalent currents feeding slots of non-resonant waveguide antennas

Solution I

The easiest solution which allows solving problem of the physical non-realizability for some amplitude distributions of the equivalent currents feeding slots of the non-resonant waveguide antennas is the modification of the loss coefficient χ_N. It is obviously connected with an increase of the power lost in the matched waveguide termination.

By the modification of the loss coefficient, for the antenna presented in chapter 2.2, to the value $\chi_N = 0.2$ (the antenna efficiency equals $\eta = 80\%$) it is possible to obtain normalized slots conductances lower than 1.0.

Slot No. k	Conductances without Internal Mutual Couplings Consideration g_k	Conductances with Internal Mutual Couplings Consideration g_k	Deviation of the phase angle from linear distribution $\delta\phi_k [^\circ]$	Displacement from waveguide axis x_k [mm]
1	0.0061	0.0032	22.55	0.36
2	0.0415	0.0291	29.80	1.10
3	0.1372	0.1483	32.52	2.53
4	0.2701	0.4631	27.52	4.71
5	0.3699	0.8020	14.92	6.67
6	0.3457	0.6131	4.17	5.58
7	0.1669	0.2052	0.51	3.01
8	0.0294	0.0303	0	1.13

Table II. Electrical and construction parameters of the designed antenna – Solution I

In Fig. 6 the equivalent voltage amplitude distribution along the feeding waveguide for the antenna with $\chi_N = 0.2$ is shown.

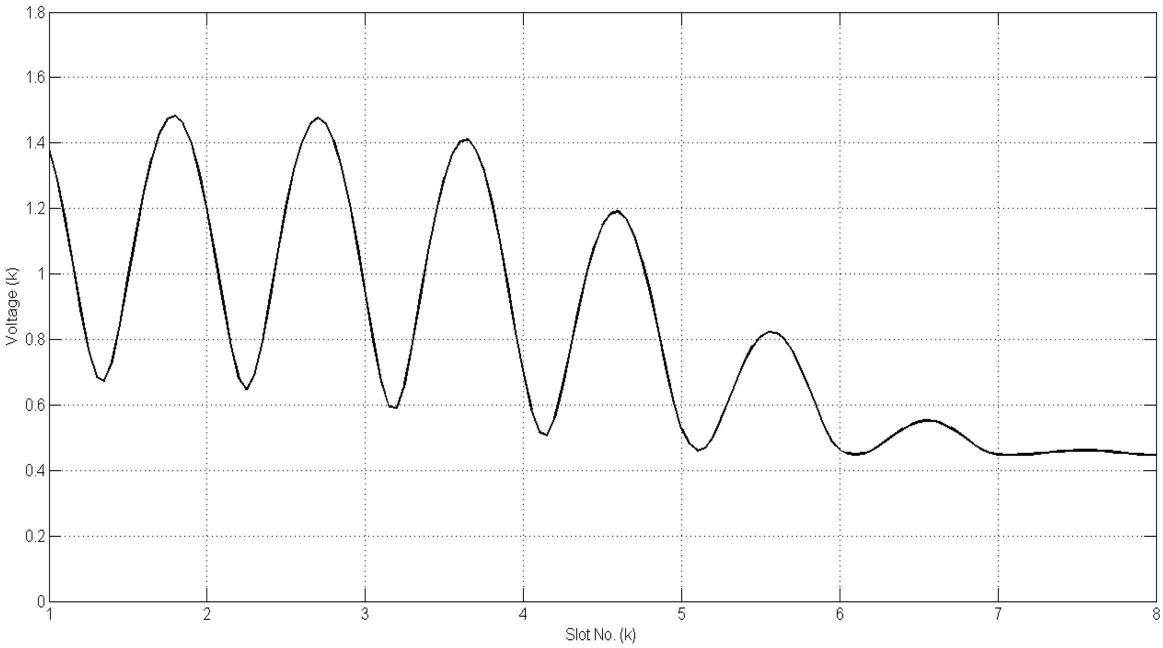

Figure 6. The equivalent voltage amplitude distribution along the feeding waveguide of the designed antenna – Solution I.

For the evaluation of oscillations caused by the wave reflections from slots, voltage distributions along the feeding waveguide for both antennas (i.e. for the antenna loss coefficient $\chi_N = 0.1$ and $\chi_N = 0.2$) were compared (see Fig. 5 and Fig. 6). It was observed that for the larger loss coefficients χ_N these amplitude oscillations are smaller. Values of slot conductance for larger loss coefficients are lower as well. According to this observation can be affirmed that for lower conductances each slot generate smaller disturbances of electromagnetic wave distribution in the feeding waveguide. This deduction is affirmed by the phase deviations from the linear distribution $\delta\phi_k$ for the both loss coefficients χ_N which are presented in Table I and Table II. These deviations are smaller for larger values of the loss coefficient as well.

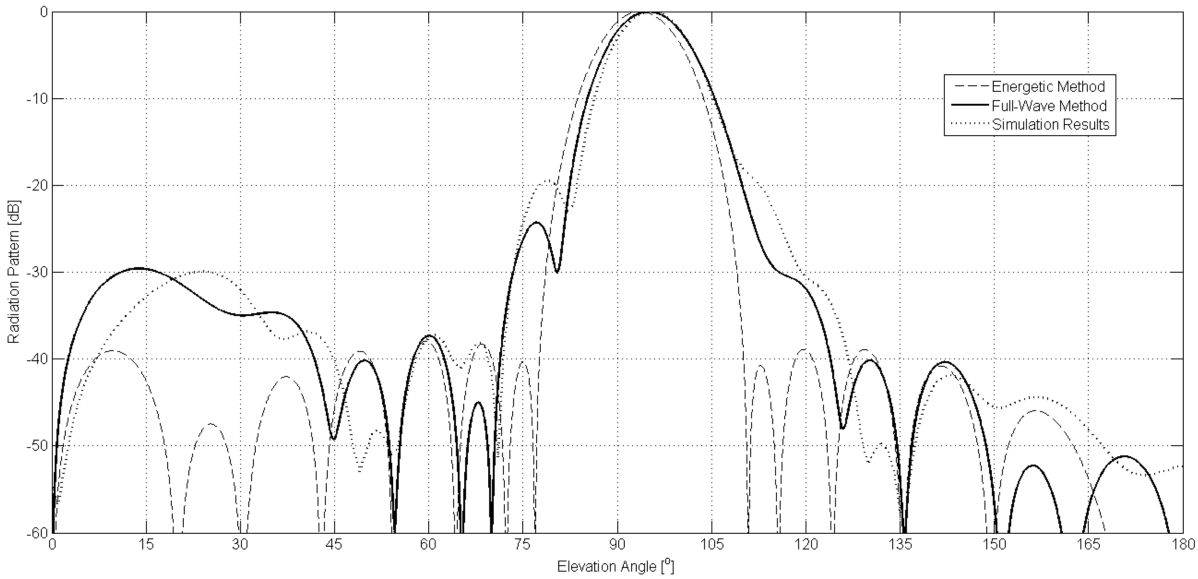

Figure 7. The radiation pattern of the designed antenna (Solution I) obtained with the Energetic Method (dashed line), the Full-Wave Method (solid line) and the CST Microwave Studio simulations (dotted line).

Comparing the radiation patterns shown in Fig. 7 observed significant differences between the Energetic and the Full-Wave Methods. These differences are caused by not considered the internal mutual couplings between slots in the Energetic Method. The most significant effects of the internal mutual couplings influence on the radiation pattern are an increase of the first sidelobes pair level and the distortion of the main lobe. Additionally the main lobe is extra squinted from the normal to the antenna aperture.

Radiation patterns obtained with the Full-Wave Method and in CST Microwave Studio simulations were also compared. The largest difference observed for the first pair of sidelobes. Differences between patterns obtained with the Full-Wave Method and the simulations are caused by the external mutual couplings between slots which are not considered in the Full-Wave and the Energetic Methods. These external mutual couplings can be evaluated by the design method presented in [7].

Solution II

The second solution is a modification of the amplitude distribution for the same loss coefficient χ_N. In order to reach the physical realizability of the antenna it is desired that the current amplitude distribution is close to the regular distribution. Such solution obviously causes increase of sidelobes level but decreases the internal mutual couplings between slots as well.

As an example parameters of the Taylor's amplitude distribution of the feeding slots currents for the antenna presented in chapter 2.2 were modified to the values: $\alpha = 1.3$ and $n = 2$ (the amplitude distribution closer to the regular distribution). For the same value of the loss coefficient $\chi_N = 0.1$ it is possible to obtain slots conductance which enable the physical realization of such antenna.

Slot No. k	Current Amplitude Distribution I_k	Conductance without Internal Mutual Couplings Consideration g_k	Conductance with Internal Mutual Couplings Consideration g_k	Deviation of the phase angle from linear distribution $\delta\phi_k\,[^\circ]$	Displacement from waveguide axis x_k [mm]
1	0.420	0.0358	0.0193	26.16	0.90
2	0.590	0.0733	0.0479	33.79	1.42
3	0.830	0.1568	0.1412	38.59	2.47
4	1.000	0.2700	0.3616	38.44	4.09
5	1.000	0.3698	0.7219	31.17	6.20
6	0.830	0.4042	0.9307	17.83	8.46
7	0.590	0.3424	0.6542	5.81	5.81
8	0.420	0.2636	0.3580	0	4.07

Table III. Electrical and construction parameters of the designed antenna – Solution II

On the basis of slots conductance values gathered in the column 4 of Table 3 it is possible to affirm that designed antenna is physically realized (conductance of all slots less than 1.0). Amplitude oscillations of the voltage distribution along the feeding waveguide for this current distribution presented in Fig. 8 are smaller than their equivalents shown in Fig. 5 (for Taylor's parameters: $\alpha = 2$ and $n = 4$). It allows to conclude that for current distributions which are closer to the regular distribution ($\alpha = 1.3$ and $n = 2$) disturbances of the electromagnetic wave distribution in the feeding waveguide caused by the internal mutual couplings are smaller.

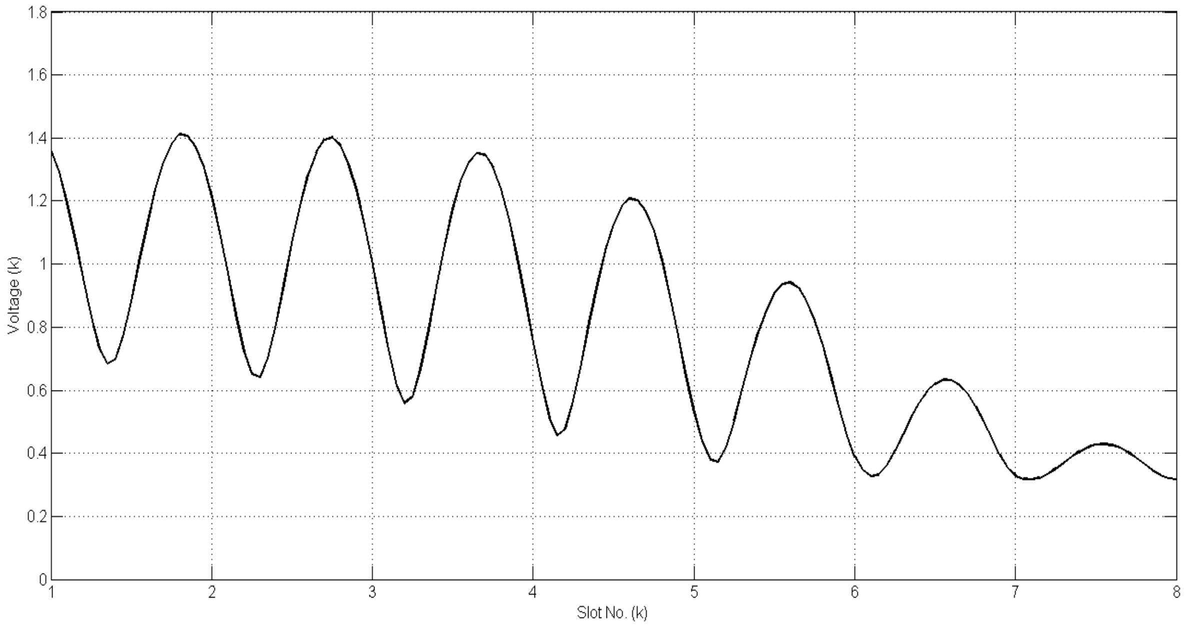

Figure 8. The equivalent voltage distribution along the feeding waveguide of the designed antenna – Solution II.

For this solution it is possible to seen the large discrepancies between the Energetic and the Full-Wave Methods results, especially for the first side lob pair (uprising their level), and also the radiating deviation from the antenna aperture (see Figure 9). The discrepancies between the Full-Wave Method and simulation results appear mainly for the first side lob level. These discrepancies are definitely smaller in the comparison to the differences between patterns obtained with the Energetic Method and the computer simulations.

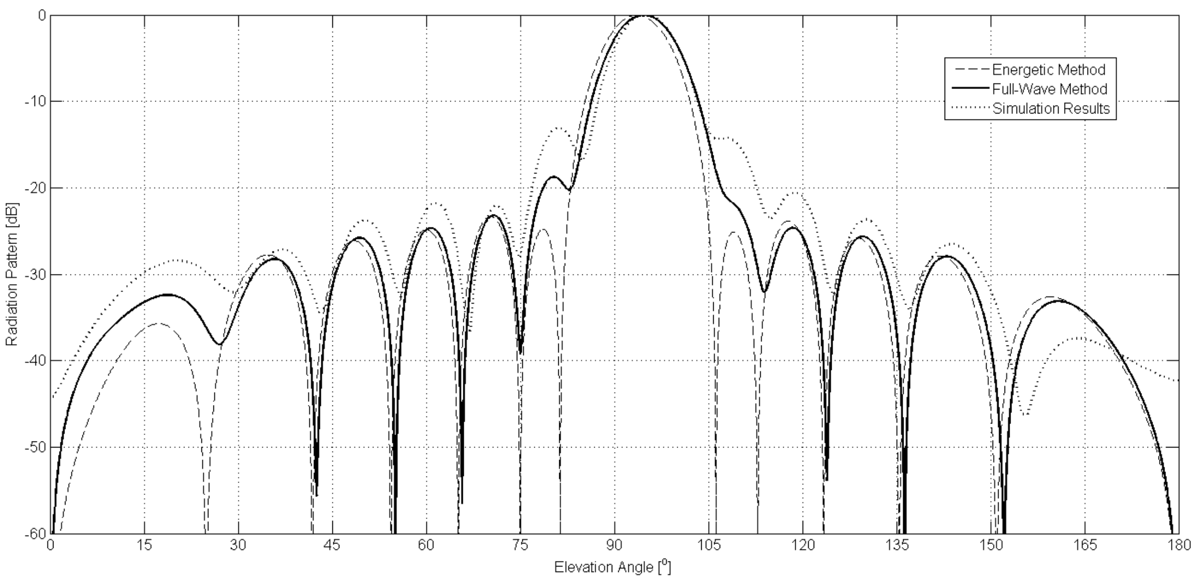

Figure 9. The radiation pattern of the designed antenna (Solution II) obtained with the Energetic Method (dashed line), the Full-Wave Method (solid line) and the CST Microwave Studio simulations (dotted line).

Solution III

The last of the proposed solutions is an increase of the radiating slots number. These solution allows to decrease the mutual couplings between particular. Main disadvantage of such solution is not only increase of dimensions and weight, but also the main lobe width contraction.

The antenna shown in chapter 2.2 after the number of slots modification is use as an example of such solution. Increasing the number of slots to 10 and leaving rest of parameters without changes makes possible to receive slots conductance values permissive for the physical realizability of such antenna.

Slot No. *k*	Current Amplitude Distribution I_k	Conductance without Internal Mutual Couplings Consideration g_k	Conductance with Internal Mutual Couplings Consideration g_k	Deviation of the phase angle from linear distribution $\delta\phi_k [^\circ]$	Displacement from waveguide axis x_k [mm]
1	0.022	0.0045	0.0021	16.74	0.30
2	0.109	0.0222	0.0118	25.71	0.70
3	0.355	0.0737	0.0486	33.32	1.43
4	0.713	0.1601	0.1470	37.94	2.52
5	1.000	0.2672	0.3690	37.34	4.14
6	1.000	0.3645	0.7385	29.08	6.30
7	0.713	0.4092	0.9413	14.95	8.54
8	0.355	0.3445	0.6085	4.34	5.55
9	0.109	0.1618	0.1993	0.68	2.96
10	0.022	0.0392	0.0408	0	1.31

Table IV. Electrical and construction parameters of the designed antenna – Solution III

Conductances obtained with the including of the internal mutual couplings between slots (column 4 Table 4) allow verifying that such antenna is fully realizable (conductances lower than 1.0). Comparing distributions shown in Fig. 10 and Fig. 5 it was noticed that oscillates of the voltage distribution for the 10-slots antenna are smaller than for the 8-slots antenna.

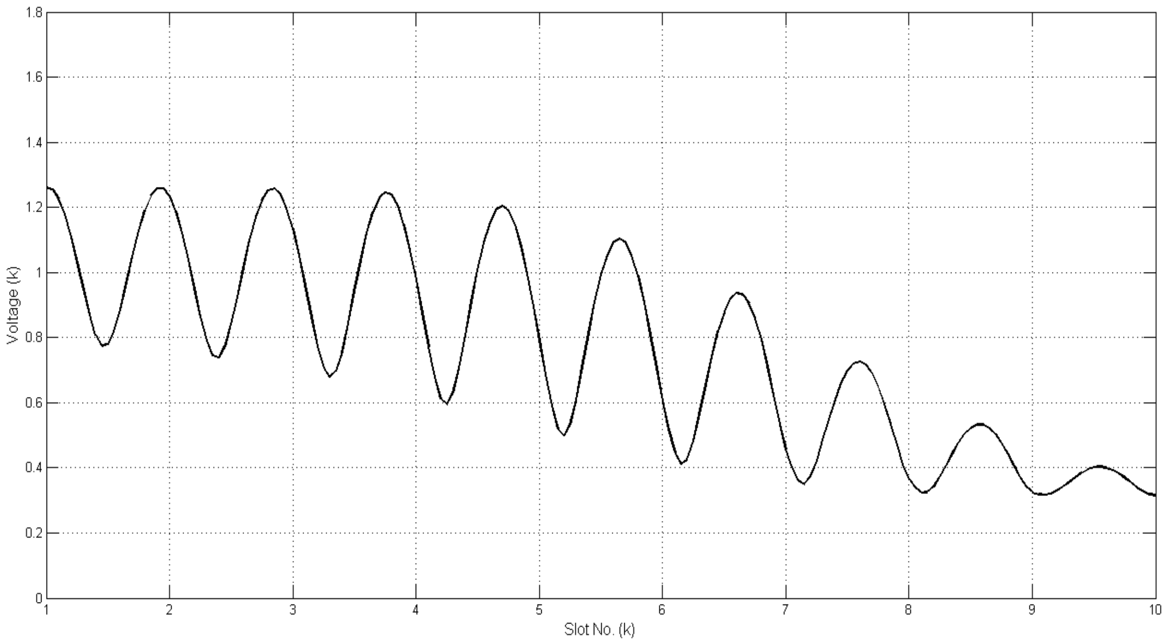

Figure 10. The equivalent voltage amplitude distribution along the feeding waveguide of the designed antenna – Solution III.

In Fig. 11 the radiation patterns obtained with the Energetic and the Full-Wave Methods and in CST Microwave Studio simulations are shown.

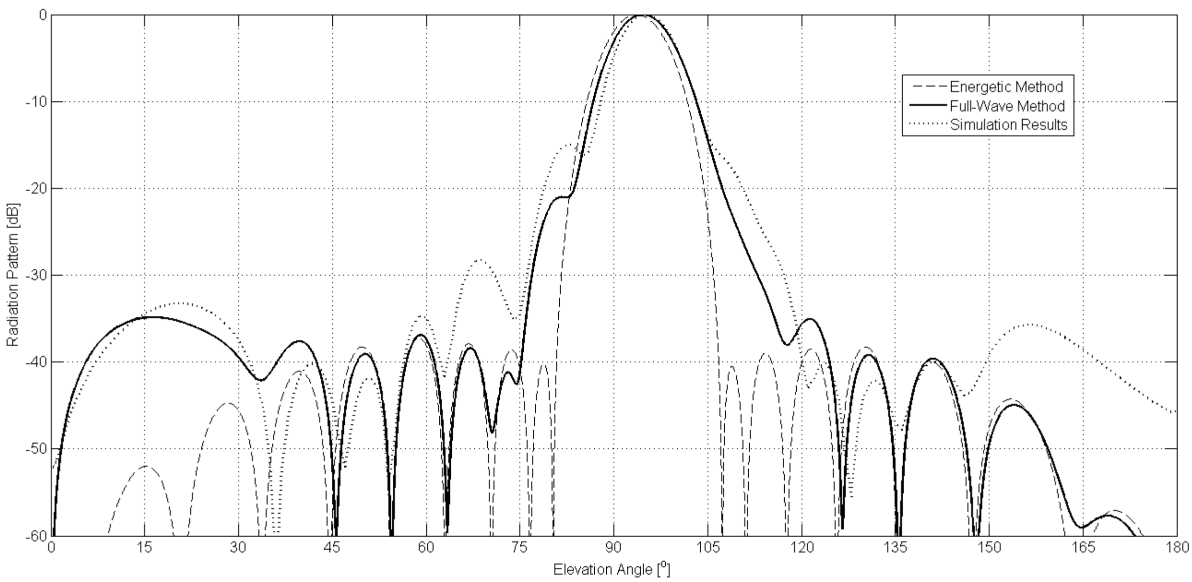

Figure 11. The radiation pattern of the designed antenna (Solution III) obtained with the Energetic Method (dashed line), the Full-Wave Method (solid line) and the CST Microwave Studio simulations (dotted line).

Comparing the radiation patterns shown in Fig. 11, it is possible to perceive the large disorders between radiation patterns obtained with the Energetic Method and the Full-Wave Method.

4 Conclusions

In this article the Full-Wave Method of the non-resonant waveguide slotted antennas design, taking the internal mutual couplings effect between slots under consideration, is presented. This method was used to design the non-resonant waveguide antenna with the 8 longitudinal slots alternating placed on both sides of the rectangular waveguide broad wall axis. Slots of this antenna were fed by currents amplitudes obtained with the Taylor's Method. Unfortunately normalized slots conductance reached with the Full-Wave Method were not physically realized. For the two centre slots obtained normalized conductance were larger than 1.0. It means that these slots should radiate larger power than the power which fed these slots. The main reason of this fact was the internal mutual coupling effect between slots. In order to enable the physical realizability of such antenna three solutions which adjusted some parameters of this antenna were presented. These solutions allowed realizing the designed antenna but the radiation pattern or the energetic efficiency of this antenna were slightly deteriorated.

In this article the influence of the internal mutual couplings between radiating slots on the radiation pattern of the non-resonant slotted waveguide antenna was also presented. This influence was estimated by the comparison of the radiation patterns obtained with the Energetic and the Full-Wave Methods. The obtained patterns were especially different for the side lobes level and the distortion of the main lobe. Additionally this effect caused an increase of the end fire angle deviation from the normal to the antenna aperture.

In order to confirm usefulness of the presented Full-Wave Method patterns obtained with this method were compared to their equivalents reached in the CST Microwave Studio simulations were compared. As it follows from the comparison of both patterns proposed the Full-Wave Method makes possible to design the non-resonant slotted waveguide antennas. Obtained patterns were in the agreement and main differences were for the level of the first side lobes level. It is worth to emphasize that this differences were much smaller than differences between patterns obtained with the Energetic Method and in the simulations.

5 References

1. Balanis C.A., ”Antenna Theory Analysis and Design”, John Wiley and Sons, New York, 1997,
2. Bem D.J. “Anteny i rozchodzenie się fal radiowych”, WNT, Warszawa, 1973, (in Polish),
3. Das B. N., Ramakrishna J.B.K., “Resonant conductance of inclined slots in the narrow wall of rectangular waveguide“, IEEE Trans., vol. 32, Antennas and Propagation, pp. 759 ÷ 761, July 1984,
4. Dion Andre, “Nonresonant slotted arrays”, IRE Trans., Antennas and Propagation, pp. 360 ÷ 365, October 1958,
5. Elliott R.S., ”The design of traveling wave fed longitudinal shunt slot arrays”, IEEE Trans., vol. 27, Antennas and Propagation, pp. 717 ÷ 720, September 1979,
6. Elliott R.S., O'Loughlin W.R., ”The design procedure of slot array including internal mutual couplings”, IEEE Trans., vol. 34, Antennas and Propagation, pp. 1149 ÷ 1154, September 1986,
7. Elliott R.S., L.A. Kurtz ”The design of small slot arrays”, IEEE Trans., vol. 26, Antennas and Propagation, pp. 214 ÷ 219, January 1978,
8. Evstropov G.A., S.A. Carapkin, ”Rasczot wołnowodno – szczelewych anten syczotom wzaimodiejstwa izłuczatielej po osnownoj wołnie”. Radiotiechnika i elektronika , AN ZSRR, t. XI , No.5 , 1966 , s. 822 ÷ 830 (in Russian),
9. Grabowski M., „Analiza i wyniki wpływu wewnętrznych sprzężeń elektromagnetycznych na charakterystyki wieloelementowych nierezonansowych anten falowodowo – szczelinowych”, Prace PIT, Warszawa 2008, (in Polish).
10. Grabowski M., „Analysis of an internal mutual couplings influence on a radiation pattern of a nonresonant multi-slots waveguide array antenna”, Conference Proceedings, MIKON-2008, Wrocław 2008.
11. Johnson R.C., “Antenna engineering handbook”, third edition McGraw-Hill, Inc. New York 1993.
12. Kaszin A.W., ”Mietody projektirowania i issledowania wołnowodno – szczelewych antennych reszotok”, Radiotechnika, Moskwa 2006, (in Russian).
13. Oliner A.A, “The impedance properties of narrow radiating slots in the broad face of rectangular waveguide; part I – theory”, IRE Trans., Antennas and Propagation, January 1957, pp. 4 ÷ 11, January 1957.

14. Powen Hsu, Shin H. Chen, “Admittance and resonant length of inclined slots in the narrow wall of a rectangular waveguide”, IEEE Trans., vol. 37, Antennas and Propagation, pp. 45 ÷ 49, January 1989.
15. Rosłoniec S., „Podstawy techniki antenowej”, Oficyna Wydawnicza Politechniki Warszawskiej, Warszawa 2006, (in Polish).
16. Rosłoniec S., „Analiza wpływu wewnętrznych sprzężeń elektromagnetycznych na charakterystyki promieniowania nierezonansowych anten falowodowych”, Prace PIT, Warszawa 2007, (in Polish).
17. Stern Geogr. J., Elliott Robert S. “Resonant length of longitudinal slots and validity of circuit representation: Theory and experiment”, IEEE Trans., vol. 33, Antennas and Propagation, pp. 1264 ÷ 1271, November 1985.
18. Stevenson A.F., ”Theory of slots in rectangular waveguides”, Journal of Applied Physics, vol. 19, pp. 24 ÷ 38, January 1948.